A. EVTUKH,[1] V. LITOVCHENKO,[1] M. STRIKHA,[1] A. KURCHAK,[1]
O. YILMAZOGLU,[2] H. HARTNAGEL[2]

[1] V.E. Lashkaryov Institute of Semiconductor Physics, Nat. Acad. of Sci. of Ukraine
   (41, Prosp. Nauky, Kyiv 03028, Ukraine; e-mail: anatoliy.evtukh@gmail.com)
[2] Department of High Frequency Electronics
   (Technische Universität Darmstadt, 64283, Darmstadt, Germany)

PACS 79.70.+q

CONDUCTIVE NANORODS IN DLC FILMS CAUSED BY CARBON TRANSFORMATION

The influence of diamond-like carbon (DLC) films deposited under various conditions on the electron field emission (EFE) of silicon (Si) tips has been investigated. During the nitrogen-doped DLC film deposition, the nitrogen content in a gas mixture is varied from 0% to 45%. In this context, the effective work function is optimized, by reaching the values less than 1 eV. A sharp increase in the emission current at high electric fields and a decrease of the threshold voltage after the pre-breakdown conditioning of a DLC film on Si tips have been measured. At high current densities and the resulting local heating, the diamond-like sp^3 phase transforms into a conducting graphite-like sp^2 phase. As a result, an electrical conducting nanostructured channel is formed in the DLC film. The diameter of the conducting nanochannel is estimated from the reduced threshold voltage after the pre-breakdown conditioning to be in the interval 5–25 nm. The presence of this nanochannel in the insulating matrix leads to a local enhancement of the electric field and a reduced threshold voltage for EFE. The obtained results can be used for the development of highly efficient field emission cathodes. To explain the experimental EFE results based on a transformation of DLC films and the generation of conduction nanochannels, the changes of the electron affinity (χ_0) for various carbon structures and impurity point defects have been calculated. The influence of the rehybridization of bonds in various carbon crystal structures on χ_0 is shown. The formation of conducting channel arrays in DLC films will allow us to significantly enhance EFE even on flat surfaces without tips.

K e y w o r d s: diamond-like carbon film, electron field emission, conductive nanorods, carbon nanotube.

1. Introduction

Carbon is a material with unique properties due to a possibility to have various allotropic forms: diamond, graphite, graphene, fullerene, and carbon nanotubes (CNTs) that have different configurations of interatomic bonds. It is worth to note that the chemical bonds can be changed during the transition between different forms of carbon. As a result, the optical, electrical, and other properties including the work function and the electron field (cold) emission are also changed.

The fabrication of efficient and stable field emission cathodes is still an important problem, in spite of the progress in vacuum microelectronics during the last decades due to the outstanding designs such as Spindt cathodes, quantum cathodes, microsize diamond, CNTs, *etc.* The efficiency of an electron field emission cathode with the DLC film on Si tips should

be compared with that of uncoated ones. According to the Fowler–Nordheim equation, the electron field emission efficiency is determined in terms of the work function (Φ) and the electric field enhancement coefficient (β). In case of Si tips coated with a thin DLC film, a significant decrease of Φ dominates in comparison with a small reduction of β. The main advantages of carbon cathodes are the low work function and the high chemical and physical stability in comparison with Si or molybdenum emitters [1].

The promising way to improve the emission properties of semiconductor and metal cathodes is their coating with carbon-based layers [1–3]. Nowadays, CNTs are good electron sources, but pose else emission stability problems.

In our previous publications, we used diamond-like carbon (DLC) films, which contained diamond and graphite phases and coated micro- or nanorelief substrates typically based on porous Si surfaces. Those structures demonstrated the enhancement of the field emission, but had no good reproducibility and stability.

Below, we will describe another cathode design based on graphite nanorods embedded in a DLC film. The graphite nanorods are conductive channels with large concentration of carriers, whereas the surrounding matrix is a DLC layer with the low work function on the top of graphite nanorods.

2. Experimental

2.1. Cathode formation

The Si emitter tips were fabricated by the wet chemical etching. The cathodes were formed on (100) Si n-type wafers ($N_d = 10^{15}$ cm^{-3}) by patterning a Si$_3$N$_4$ mask. The additional tip sharpening was performed by the oxidation of the as-etched tips at 900 °C in wet oxygen. After the oxidation, the oxide is removed into an HF : H$_2$O solution. This sharpening technique allows the production of tips with a radius curvature of 10–20 nm. The height of the Si tips was 4 μm. The array size and the tip density were 8×8 cm^2 and 2.5×10^5 tips/cm^2, respectively. The radii before and after the DLC film deposition were estimated by the scanning electron microscopy (SEM).

DLC films with various thicknesses in an interval of 60-80 nm were grown on flat Si wafers and Si tip arrays by the plasma enhanced-chemical vapor deposition (PECVD) method from a CH$_4$: H$_2$: N$_2$

mixture. We excluded the effect of small film thickness variations on the emission parameters. The nitrogen content in the gas mixture was varied from 0% to 45%. The *in situ* gas-phase doping allowed us to deposit DLC films with different nitrogen contents. These DLC films were deposited under three different levels of gas pressure in the chamber: 0.2, 0.6, and 0.8 Torr. The substrates were put directly on a water-cooled cathode ($\oslash$200 mm) which was capacitively connected to a 13.56-MHz generator. During the plasma deposition, the radio-frequency (rf) bias voltage was about 1900 V. The DLC coatings were smooth and had reproducible properties from sample to sample under the same deposition conditions.

2.2. Measurements

The emission current was measured in the ungated cathode-anode diode configuration in a vacuum system at 10^{-6} Torr. The emitter-anode spacing L was 20 μm. A Si wafer with DLC coated Si tips was used as a cathode, and a highly doped Si wafer or quartz plate coated with indium–tin–oxides (ITO) was used as an anode. A 20-μm-thick teflon spacer was used to keep the two plates separated from each other. The emission current–voltage characteristics were obtained with a current sensitivity of 5 nA over a voltage range up to 1500 V. A 0.56 MΩ resistor was placed in series with the cathode to provide the short-circuit protection.

The tip array was etched on a 8×8 cm^2 wafer, diced in 1 cm^2 squares and mounted in a vacuum station. These test Si tip arrays without coating were dipped in a 5% HF solution for 20 s to remove the native oxide layer immediately before the mounting in the high-vacuum system. The investigated cathode area was 5.5×10^{-3} cm^2 and contained 1.4×10^3 tips. Flat Si wafers were used to determine the thickness/refractive index of the DLC films and the nitrogen content with a laser ellipsometer ($\lambda = 632.8$ nm) and the Auger electron spectroscopy, respectively.

3. Results and Discussion

3.1. Influence of technological conditions on DLC film properties

The EFE current–voltage characteristics of the Si tip arrays coated with undoped and nitrogen-doped DLC
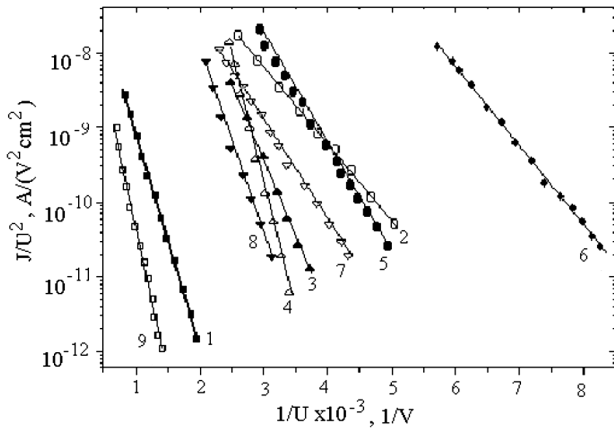
Fig. 1. Emission current–voltage characteristics in the Fowler–Nordheim coordinates for pure Si tips (*1*) and Si tips with N_2-doped DLC films (*2–9*): $C(N_2) - 0\%$ (*2*); 5% (*3*); 15% (*4*); 20% (*5*); 25% (*6*); 30% (*7*); 35% (*8*); 40% (*9*). $C(N_2)$ is the nitrogen content in a gas mixture under the PE-CVD deposition
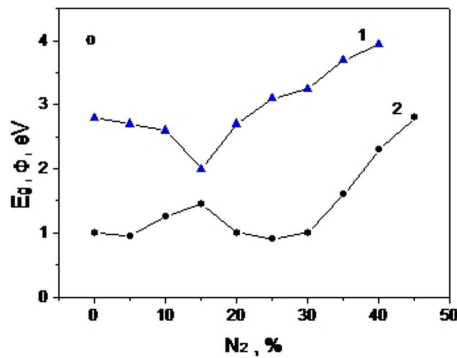

Fig. 2. Band gap (*1*) and work function (*2*) of DLC films vs. the nitrogen content in a gas mixture. The work function of pure Si tips is given with "o"

films in the Fowler–Nordheim (F–N) coordinates are presented in Fig. 1.

The curves are straight lines over a wide field range. The F–N plots were used to determine the threshold voltage, work function, field enhancement coefficient, and effective emission area according to the procedure described in Refs. [3–5]. It is not possible to determine the field enhancement coefficient (β) and work function (Φ) from the F–N plot alone. The field enhancement coefficients were calculated from the geometry of the emitting system according to the relation

$$\beta = h/(r + d), \tag{1}$$

where r is the radius of a tip estimated with SEM, h is the height of a tip, d is the thickness of a DLC film. In the case of Si tips without DLC coatings, the field enhancement coefficient was determined from the F–N plot at the work function of Si $\Phi = 4.15$ eV. A good agreement was obtained between β calculated from Eq. (1) with $d = 0$ ($\beta \approx 200$) and determined from the F–N plot ($\beta \approx 230$). The work functions for different DLC film coatings were determined from the slope (b) of the F–N plot, by using the calculated β coefficient. The ratio of the work functions of the pure Si tip and the Si tip coated with a DLC film is

$$\Phi/\Phi = (b_1\beta_1/b_2\beta_2)^{2/3}, \tag{2}$$

where Φ_i is the work function, β_i is the field enhancement coefficient, and b_i is the slopes in the F–N plot, with $i = 1$ for the Si tip and $i = 2$ for the Si tip with a DLC coating. The field enhancement factor is mainly determined by the radius curvature of Si tips, which is approximately the same for all DLC-coated Si tip arrays. However, the threshold voltage, effective work function, and emission area depend on the nitrogen content in the DLC film.

The dependence of the work function on the N_2 content in the gas mixture is presented in Fig. 2 (curve *2*). For comparison, the work function of the pure Si emitter without DLC coatings is shown. A nonmonotonous dependence is observed. There is a growth of the work function in the initial part of the curve. A further increase of the N_2 content caused a decrease of Φ. At high N_2 concentrations, Φ increased again. The lowest value of $\Phi = 0.92$ eV was obtained for a DLC film deposited at the 25-% N_2 content in a gas mixture. The influence of the gas pressure on the effective work function is significant. The optical band gap of the DLC films was measured, by using the spectroscopic ellipsometry. The band gap changed significantly with the N_2 content in the DLC film, where the smallest value of E_g was 2 eV at the 25-% N_2 content, and the largest value was 4 eV at the ~40-% N_2 content (Fig. 2 (curve *1*)). Our experimental results concerning the influence of the nitrogen doping on DLC film properties are in agreement with the data obtained in [1].

For the qualitative explanation of the experimental results, we refer to the model of DLC film as a diamond-like (sp^3 bonds) matrix with graphite-like inclusions in it. According to Ref. [6], the carbon atoms at sp^2 sites tend together in aromatic

rings, forming graphite-like islands. Nitrogen atoms in DLC films stabilize carbon atoms at sp^3 sites with the C–N bond creation. At the same time, nitrogen is a donor-type impurity in diamond and DLC films. The undoped DLC film shows the p-type conductivity. Under low levels of nitrogen doping in DLC, the n-type donor impurity compensates the p-type one. As a result, the conductivity of a DLC film is decreased [1]. When the N content is less than 1.7%, the emission current is less than that of an undoped DLC film, probably, due to the higher resistance of the compensated DLC film.

The continuous shift of the Fermi level toward the conduction band occurs with a growth of the N content in the film. This causes an increase in the emission current and a decrease of the threshold voltage. The effective work function decreases, but a further growth of the N content promotes an increase of the band gap [see Fig. 2 (curve *2*)] due to the sp^3 bond growth. Consequently, the effective work function is increased. As a result, the dependence of the effective work function on the N content has a minimum. According to the model of DLC films as a diamond-like matrix with graphite-like inclusions in it, these films are not homogeneous, and their thickness and structural heterogeneity depend on the deposition conditions.

The nonmonotonous dependences of E_g (Fig. 2 (curve *2*)) on the nitrogen content in a gas mixture may be interpreted in the framework of a model involving the effect of nitrogen on the film structure. At low concentrations, the nitrogen atoms fit into the film at sp^2-clusters boundaries, by increasing the fraction of the disordered sp^2 phase [7, 8]. This must result, in turn, in a decrease of E_g, which is actually observed [see Fig. 2 (curve *2*)]. As the nitrogen content in the film further increases, the excess nitrogen atoms begin to fit in between the sp^2 clusters. This causes the strain relaxation in the film and stimulates the formation of sp^3-coordinated carbon–hydrogen bonds. As this takes place, E_g increases.

3.2. Formation of conducting nanochannels

In some cases, the peculiarities of EFE from DLC-coated metals or semiconductors can be explained, by assuming that there is a structure on the film surface (and, hence, an external field enhancement), or
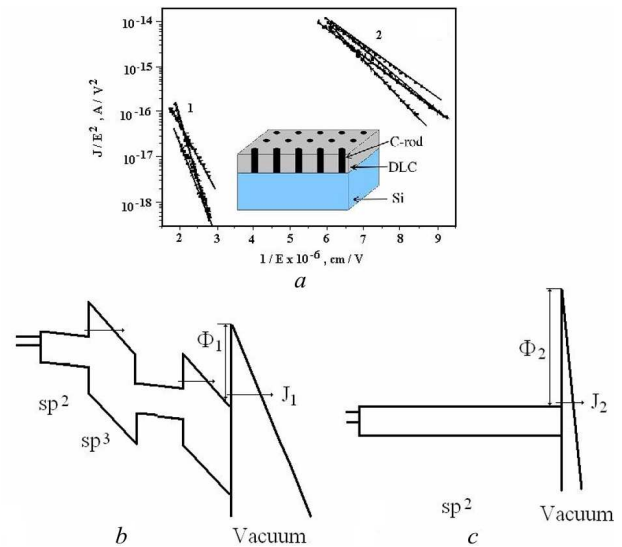

Fig. 3. (*a*) Fowler–Nordheim emission characteristics from Si tips coated with a DLC film before (*1*) and after (*2*) the pre-breakdown conditioning. The set of subsequent measurements is included (in the insert: the schematic image of formed nanochannels). Energy band diagrams of Si tips coated with a DLC film before (*b*) and after (*c*) the formation of conducting nanochannels ($\Phi_1 < \Phi_2$, $\beta_1 < \beta_2$, $J_1 < J_2$)

a structure inside the film (internal field enhancement), or a combination of both (hybrid field enhancement). Both hybrid and internal field enhancements may operate at different locations on the same film. In Ref. [9], such DLC films were determined as partially graphite-like (PGL) films. EFE that can be explained by the emission model based on the cluster model of a DLC film was observed in Ref. [1]. But in the EFE investigations, the effects of a sharp growth of the emission current and a decrease of the threshold voltage in the repeating measurements at high electric fields were revealed after the DLC film conditioning. These effects are realized after the DLC film deposition on Si tips (Fig. 3).

The barriers caused by the sp^3 phase between sp^2 inclusions can be broken during the EFE at high-electric fields. At the DLC film breakdown and the flow of a high current, the local heating is possible, and the transformation of the sp^3 phase into the sp^2 one can occur. As a result, the conducting channel between the Si substrate and the DLC film surface is created. Electrically nanostructured heterogeneities are formed at the pre-breakdown. The schematic energy band diagrams of Si tips coated with

a DLC film before and after the pre-breakdown conditioning are shown in Fig. 3 (*b*, *c*).

The existence of conducting channels in the dielectric (semiconductor) matrix with possible nanometer-sized clusters of the sp^2 phase on the surface forms the internal tip in the DLC film, and the additional local enhancement of the electric field appears and promotes the EFE. The detailed analysis of EFE peculiarities from electrically nanostructured heterogeneous materials is given in Ref. [9]. In Ref. [10], the results of experiments with DLC films deposited by the laser ablation with the use of a conductive AFM probe have been reported. It was shown that the field-induced electron emission sites are associated with small morphological features (inclusions) on the film front surface. These sites exhibit the high conductivity between the probe and the underlying substrate. In films with a high sp^2 content, these features are found without any need to activate the film. For a film with a low sp^2 content, the initially insulating and flat inclusions could be found only after the film activation by a vacuum-arc discharge between the film and the counter electrode, as described in Ref. [1]. It was assumed that the observed increase of the conductivity (by at least two orders of magnitude) can only be explained by the formation of conductive channels through the whole thickness of the film down to the Si substrate. They assumed that the surface inclusions (and the channels) have been created by the transformation of sp^3 bonding to conducting sp^2-bonded carbon. For the films with a high sp^2 content, they assumed that channels already exist or can be formed by applying a field without the need for the arc-based activation process. Like a freestanding conductive tip in vacuum, a conductive channel in the insulating matrix leads to a field enhancement and the enhanced electron emission.

The defects create local energy states in the bandgap of the sp^3 phase and increase its conductivity in such a way. Referring to the mentioned processes of sp^3 phase graphitization and defect creation, two types of conducting channels between the substrate and the DLC film surface can be considered. The first one (type I) is a conductive graphite (graphite-like) channel formed as a result of the transformation of the sp^3 phase into the sp^2 one. The second type (type II) of a conduction channel is based on a conductivity increase of the sp^3 phase due to structure defects' generation between sp^2 phase inclusions in the DLC film. For this channel type, the surface of the film consists of a diamond-like sp^3 phase, which has a significantly lower work function in comparison to graphite. Values less than 1 eV have been reported in [11].

From the F–N plots, we can determine the effective work function $\Phi^* = \Phi/\beta^{2/3}$ (Φ is the work function of DLC, β is the field enhancement coefficient). The obtained effective work-function values before and after the conditioning are $\Phi_1^* = 1.1 \times 10^{-1}$ eV and $\Phi_2^* = 4.1 \times 10^{-2}$ eV, respectively. They are in agreement with values reported in [1]. For the used Si tips ($r = 10$ nm, $h = 4$ μm) and DLC coating thickness ($d = 60$ nm), a work function of 1.63 eV before the pre-breakdown conditioning has been calculated. In the case of a DLC film, Φ does not denote the real work function, but the electron affinity. The field enhancement coefficient was estimated from relation (1) that includes the geometrical parameters. The obtained value of β was 58. The conducting channel diameter was calculated for type I and type II channels. In the first case, the work function $\Phi \approx 5$ eV for graphite was used. Values of conducting channel diameter in the interval 5–9 nm were obtained. For type II, a lower work function of the DLC film was used ($\Phi = 1.63$ eV). A channel diameter of about 25 nm was obtained. These channel diameter values for type I and type II are in good agreement with the size of the sp^2 phase inclusion in the sp^3 phase matrix [9, 12, 13] and with the model proposed in [9, 14]. It cannot be excluded that the work function of a DLC film on the surface is also changed. In this case, the channel diameter will be taken between 5 and 25 nm. The formation of conducting channel arrays in DLC films will allow us to get a significantly enhanced EFE even on flat surfaces without tips.

3.3. Modeling

The calculations of the electron affinity χ_0 involving the structural point defects, as well as some atoms of impurities in the graphite and DLC ultrathin films, were performed by the creation of hybride configurations with regard for the energies of s and p valence orbitals and a change of the interatomic distances [15–17]. To calculate this parameter, the following formulas, which include the energy of valence bond V_v, the energy of metallic bond V_m, the energy of ionic bond V_i, as well as the geometrical parameter (the size of

a cluster), have been used [15–17]:

$$E_g = E_c - E_\nu = K \, (V_\nu^2 + V_i^2)^{1/2} \times$$
$$\times (1 - V_m^{3D}/V_\nu^{3D}) \, (L_D/L_i)^2, \qquad (3)$$

where L_D is the diamond lattice constant, and L_i is the modified carbon lattice constant.

For elements with small electric negativity, where the ionic addend can be neglected, expression (3) in the 3D case can be rewritten as follows:

$$E_g^{3D} = K \, V_\nu^{3D} \, (1 - V_m^{3D}/V_\nu^{3D}) \, (L_D/L_i)^2, \qquad (4)$$

where $V_\nu = \eta \hbar^2/m^* r_[ab]^2 \propto C/L_i^2$, $V_m = -11/4(\varepsilon_p - \varepsilon_s)$. The corresponding value of atomic terms ε_s and $\pi \varepsilon_p$ for different structures were tabulated in [15].

Calculations of the electron affinity have been made with the use of the semiempirical relation between χ_0 and E_g, which was proved for many types of crystal structures [18] and can be written as follows:

$$E_g + \chi_0 = 5.5 \text{ eV} + \Delta E_\nu(L_i), \qquad (5)$$

where ΔE_ν have value from 0 to 1, whereas L changes from L_D to L_G (where L_G is the graphite lattice constant) [18].

For DLC mixed films, a decrease of E_g has been obtained in the case of 1 or 2 monolayers of atoms by the substitution of an impurity up to the transformation into 2D hexagonal structures (in plane) or

Table 1. **Calculated values of the energy gap (E_g), electron affinity ($\chi_0 = 5.5$ eV $- E_g(L)$), and experimental sp^3/sp^2 ratio of DLC films with different hydrogen (H) and vacancy (V) defects**

Parameter	Diamond	C_4H_1	C_3H_2	C_2H_3	C_4V_1	C_3V_2	C_2V_3
E_g, eV	5.5	4.6	3.49	1.98	2.85	2.14	1.42
χ_0, eV	0	0.9	2.01	3.52	2.65	3.36	4.08
sp^3/sp^2, %	100	83	72	64	69	64	55

Table 2. **Calculated values of the energy gap (E_g) and electron affinity χ_0 (in eV) for different clusters in graphite (V)**

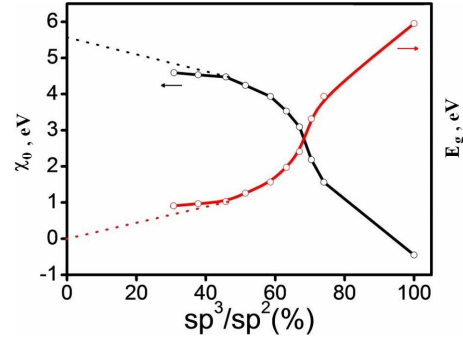| Para-meter	C_4	C_3N_1	C_2N_2	C_3H_1	C_2H_2	C_3Si_1	C_2Si_2	C_3V_1	C_2V_2
E_g, eV	5.08	5.26	5.43	3.8	2.09	4.15	3.49	3.44	1.72
χ_0, eV	0	–0.18	–0.35	1.28	2.99	0.93	1.59	1.64	3.36

Fig. 4. Energy bandgap and electron affinity vs. the sp^3/sp^2 bond ratio in DLC

with some partial configurations of sp^2 and sp^3 (as is illustrated in Table 1).

In the case of a 2D hexagonal structure, the substitution of C atoms in plane changes (increases) χ_0 in the plane direction, while the substitution normal to the plane decreases χ_0 for graphite due to a partial reconstruction of the plane with appearing partly the sp^3 hybridization due to a worsening of the surface plane (Fig. 4, Tabl. 2).

So, using partly the rehybridization of the bonds in different carbon crystal structures, it is possible to decrease χ_0 and increase electron field emission current.

4. Conclusions

The influence of undoped and *in situ* nitrogen-doped DLC film coatings on the electron field emission from Si tip arrays and flat Si wafers has been investigated in detail. To change the doping level, the concentration of nitrogen in a gas mixture used for the PECVD was changed. The emission current–voltage characteristics showed a good fit to the F–N equation. The effective work functions and field enhancement coefficients were determined and compared. The non-monotonous dependences of the effective work function and the band gap on the nitrogen content in DLC films were observed. The minimum effective work function was found to be 0.92 eV in the case of 25% of N_2 in a gas mixture. We have proposed an explanation of the experimental results with regard for the work function, band gap, and conductivity. Using a Si tip array coated with undoped and *in situ* nitrogen-doped DLC films led to an increase of electron emission currents in comparison with uncoated arrays.

An enhancement of the EFE efficiency from Si tips after the pre-breakdown conditioning of DLC films at high electric fields has been observed and explained. The high-conductive graphite-like nanochannels formed at the pre-breakdown conditioning can be applied as efficient and stable electron emitters in vacuum. As can be estimated, the conducting nanochannel diameter can be in the interval between 5 and 25 nm.

The theoretical calculation confirmed the influence of the rehybridization of bonds in different carbon crystal structures on the electron affinity.

1. V. Litovchenko, A. Evtukh. *Vacuum nanoelectronics.* In *Handbook of Semiconductor Nanostructures and Nanodevices, V. 3. Spintronics and Nanoelectronics.* Edited by A.A. Balandin, K.L. Wang (American Scientific Publishers, 2006) p. 153–234.
2. R.B. Marcus, T.S. Ravi, T. Gmitter, H.H. Busta, J.T. Niccum, K.K. Chin, D. Liu. Atomically sharp silicon and metal field emitters. *IEEE Trans. Electron Devices* **38**, 2289 (1991).
3. D.W. Branston, D. Stephany. Field emission from metal-coated silicon tips. *IEEE Trans. Electron Devices* **38**, 2329 (1991).
4. V.G. Litovchenko, A.A. Evtukh, R.I. Marchenko, N.I. Klyui, V.A. Semenovich. The enhanced field emission from microtips covered by ultrathin layers. *J. Micromech. Microeng.* **7**, 1 (1997).
5. I. Brodie, C.A. Spindt. Vacuum microelectronics. *Adv. Electron. Electron Phys.* **83**, 1 (1992).
6. J. Robertson. Structural models of a-C and a-C:H. *Diamond Relat. Mater.* **4**, 297 (1995).
7. F. Demichelis, X.F. Rong, S. Schreiter, A. Tagliaferro, C. De Martino. Deposition and characterization of amorphous carbon nitride thin films. *Diamond Relat. Mater.* **4**, 361 (1995).
8. N.I. Klyui, B.N. Romanyuk, V.G. Litovchenko, B.N. Skarban, V.A. Mitus, V.A. Semenovich, S.N. Dub. Nitrogen-doped DLC-films: Correlation between optical and mechanical properties. *J. Chem. Vapor Dep.* **5** (4), 310 (1997).
9. R.G. Forbes. Low-macroscopic-field electron emission from carbon films and other electrically nanostructured heterogeneous materials: Hypotheses about emission mechanism. *Solid State Electr.* **45**, 779 (2001).
10. O. Gröning, O.M. Küttel, P. Gröning, L. Schlapbach. Field emission from DLC films. *Appl. Surf. Sci.* **111**, 135 (1997).
11. A.A. Evtukh, V.G. Litovchenko, N.I. Klyui, R.I. Marchenko, S.Yu. Kudzinovski. Properties of plasma enhanced chemical vapor deposition diamond-like carbon films as field electron emitters prepared in different regimes. *J. Vac. Sci. Technol. B* **17**, 679 (1999).
12. V.G. Litovchenko, A.A. Evtukh, Yu.M. Litvin, M.I. Fedorchenko. The model of photo- and field electron emission from thin DLC films. *Mater. Sci. Eng. A* **353**, 47 (2003).
13. J. Robertson. Diamond-like amorphous carbon. *Mater. Sci. Eng. R* **37**, 129 (2002).
14. O. Gröning, O.M. Küttel, P. Gröning, L. Schlapbach. Field emitted electron energy distribution from nitrogen-containing diamondlike carbon. *Appl. Phys. Lett.* **71**, 2253 (1997).
15. W.A. Harrison. *Electronic Structure and the Properties of Solids* (Freeman, 1980) [ISBN: 0486660214].
16. V. Litovchenko. Determination of the base parameters of semiconductor cubic crystals via the lattice constant. *Ukr. J. Phys.* **50**, 1175 (2005).
17. V. Litovchenko, A. Kurchak, M. Strikha. The semi-empirical tight-binding model for carbon allotropes "between diamond and graphite". *J. Appl. Phys.* **115**, 243705 (2014).
18. V. Litovchenko. Analysis of the band structure of tetrahedral diamondlike crystals with valence bonds: Prediction of materials with superhigh hardness and negative electron affinity. *Phys. Rev. B* **65**, 153108 (2002).

А. Євтух, В. Литовченко, М. Стріха,
А. Курчак, О. Ілмазоглі, Г. Хартнагел

ПРОВІДНІ НАНОСТЕРЖНІ В АПВ ПЛІВКАХ, ЗУМОВЛЕНІ ТРАНСФОРМАЦІЄЮ ВУГЛЕЦЮ

Р е з ю м е

Досліджено вплив алмазоподібних вуглецевих (АПВ) плівок, осаджених на кремнієві вістря при різних умовах на польову емісію електронів. Під час осаджування суміш азоту в газовій камері змінювалась від 0 до 45%. Оцінки величини роботи виходу досягали значень, менших від 1 еВ. Спостерігалось різке збільшення струму емісії при великих значеннях електричного поля і зменшення бар'єра після досягнення передпробійних умов для АПВ плівок на кремнієвих вістрях. При великій густині струму в результаті локального нагріву алмазоподібна sp^3-фаза перетворюється в провідну sp^2-фазу. Внаслідок цього в АПВ плівках утворюються провідні наноструктуровані канали. Діаметр провідних наноканалів було оцінено зі зменшення бар'єра після досягнення передпробійних умов і він змінювався в діапазоні від 5 до 25 нм. Наявність таких наноканалів в діелектричній матриці приводить до локального зростання електричного поля і зменшення бар'єра для електронної польової емісії. Для пояснення експериментальних результатів польової емісії, базуючись на трансформації алмазоподібних плівок і утворенні провідних наноканалів, було розраховано зміну електронної спорідненості (χ_0) для вуглецевих структур з включеннями різної кількості точкових дефектів. Показано вплив регібридизації зв'язків у різних вуглецевих структурах на електронну спорідненість (χ_0) і відповідно на роботу виходу. Утворення провідних наноканалів в АПВ плівках дозволяє значно збільшити польову емісію навіть для плоских поверхонь без гострій. Отримані результати можуть бути використані для розробки високоефективних емісійних катодів.